

# Orthogonality Catastrophe in Parametric Random Matrices

Raúl O. Vallejos<sup>1,2</sup>, Caio H. Lewenkopf<sup>1</sup>, and Yuval Gefen<sup>3</sup>

<sup>1</sup> *Instituto de Física, Universidade do Estado do Rio de Janeiro,  
R. São Francisco Xavier 524, 20559-900 Rio de Janeiro, Brazil*

<sup>2</sup> *Centro Brasileiro de Pesquisas Físicas,*

*R. Dr. Xavier Sigaud 150, 22290-180 Rio de Janeiro, Brazil*

<sup>3</sup> *Department of Condensed Matter Physics, The Weizmann Institute of Science,  
Rehovot 76100, Israel*

(November 4, 2018)

We study the orthogonality catastrophe due to a parametric change of the single-particle (mean field) Hamiltonian of an ergodic system. The Hamiltonian is modeled by a suitable random matrix ensemble. We show that the overlap between the original and the parametrically modified many-body ground states,  $S$ , taken as Slater determinants, decreases like  $n^{-kx^2}$ , where  $n$  is the number of electrons in the systems,  $k$  is a numerical constant of the order of one, and  $x$  is the deformation measured in units of the typical distance between anticrossings. We show that the statistical fluctuations of  $S$  are largely due to properties of the levels near the Fermi energy.

PACS numbers: 73.23.-b, 71.10.-w, 73.23.Hk

## I. INTRODUCTION

The Anderson orthogonality catastrophe (AOC), introduced by Anderson in 1967<sup>1</sup>, is a fundamental effect observed in many-body systems. The original work addressed the ground state of a finite system consisting of  $N$  non-interacting electrons. Upon the introduction of a localized perturbation, this ground state gets modified. Anderson has shown that the overlap between the original and the modified  $N$ -electron ground states,  $\langle \Psi_N | \Psi'_N \rangle$ , is proportional to a negative power of  $N$ , and vanishes in the thermodynamic limit, hence the catastrophe. Variants of the AOC are at the basis of some central themes in solid state physics, including the x-ray edge singularity, zero-bias anomalies in disordered systems and tunneling into quantum Hall systems.

The applicability of this concept and attempts to extend it to more generic circumstances have been at the focus of attention for more than three decades. Particularly appealing is the application of AOC ideas to the field of mesoscopics. The study of mesoscopic systems involves finite size systems where it is usually important to account for the dynamics and the thermodynamics of the electrons on a quantum-mechanical level. Important ingredients in characterizing mesoscopic electronic systems include the strength of the ambient disorder potential, the system's size and shape and the strength of the electron-electron interaction. Evidently, in most cases such systems are too complex to be described or analyzed exactly. In such situations one needs to resort to various approximation schemes.

Finite size ("zero-dimensional") conductors, a.k.a. quantum dots (QDs) have received special attention in recent years, partly due to the rich physics involved, but also due to their experimental accessibility<sup>2-4</sup>. The simplest scheme to account for a QD with interacting elec-

trons is the *constant interaction* model<sup>5</sup>. The latter implies that the system Hamiltonian is given by

$$H = H_0 + H_{CI} , \quad (1)$$

where  $H_0$  is the single-particle Hamiltonian and the interaction, represented by an infinite wavelength (zero mode), is given by

$$H_{CI} = \frac{e^2}{2C} (\hat{N} - N_0)^2 . \quad (2)$$

Here  $C$  is the total effective capacitance of the dot,  $\hat{N}$  is the particle number operator, and  $N_0$  represents a tunable background charge (related to the gate voltage). For a complex QD with diffusive disorder or with chaotic dynamics, the single-particle energy spectrum and eigenfunctions of  $H_0$  should be the subject of a statistical description. It turns out that for such systems spectral correlations within energy windows up to the Thouless energy,  $E_{Th}$ , are well described by the random matrix theory (RMT), see for instance Refs. 6,7. The individual wavefunctions, hence spectral correlations, remain unchanged as we add/remove electrons from the system. Other than the Coulomb gap, we do not expect any signature of the AOC.

For various reasons the constant interaction model does not provide a satisfactory framework to account for key phenomena. The latter include some features of the addition spectrum, Coulomb peak-height correlations and electron scrambling (see e.g. Ref. 3). To improve on that model one can employ the best effective single-particle approach, the Hartree-Fock (HF) approximation. Expressed in the basis of the exact eigenstates of  $H_0$ , denoted by  $\{\psi_\alpha\}$  with the corresponding eigenenergies  $\{\varepsilon_\alpha\}$ , the HF Hamiltonian reads

$$H_{\text{HF}} = \sum_{\alpha} \varepsilon_{\alpha} \hat{n}_{\alpha} + \frac{1}{2} \sum_{\alpha, \beta} v_{\alpha\beta\alpha\beta} \hat{n}_{\alpha} \hat{n}_{\beta}. \quad (3)$$

Here  $v_{\alpha\beta\alpha\beta}$  are the antisymmetrized matrix elements of the interaction and  $\hat{n}_{\alpha}$  is the number operator of the state  $\psi_{\alpha}$ . Note that  $H_{\text{HF}}$  includes only diagonal interaction matrix elements (in the exact eigenstate basis); for a short-ranged interaction it has been shown that off-diagonal matrix elements are parametrically small.<sup>8–10</sup> It is clear that within this approximation the effective single-particle states (but not the HF energies!) are independent of the occupations of these states, and are unchanged upon the addition/removal of electrons from the system. This is in line with the Koopmans' picture.<sup>11</sup>

Only when the single-particle states of the system are modified upon the introduction of a “perturbation”<sup>12</sup> is it meaningful to address the question of the AOC. Here the perturbation can be understood as varying a localized gate voltage<sup>13</sup>, introducing a static impurity or adding an electron to the  $(N + 1)$ -st state. The latter motivates the study of

$$S = \langle \Psi_{N+1} | c_{N+1}^{\dagger} | \Psi_N \rangle, \quad (4)$$

where  $|\Psi_N\rangle$  is the  $N$ -electron system ground-state and  $c_{N+1}^{\dagger}$  is the corresponding electron creation operator at its first single-particle excited state. In all these examples (including the HF scheme) both ground states are given by Slater determinants. Indeed the Anderson formalism deals with the overlap of two Slater determinants. More specifically, one of the applications we have in mind is the role of AOC in the electronic transport through complex quantum dots. At very low temperatures their conductance peak heights in the Coulomb blockade regime can be evaluated from the tunneling rates to and from the corresponding many-body ground state of the electron island<sup>14</sup>. In the simplest approximation, these rates are given by the overlaps between a single-particle wave function in the dot and the channel wave functions. However, if interactions are taken into account, even in a HF mean field approximation, a many-body contribution to the tunneling rates has to be considered. *A priori* the inclusion of an additional electron to the island may change each individual single-particle orbital negligibly; however, if the number of electrons in the dot is large enough, the new many-body ground state can be almost orthogonal to the old one. Some aspects of the AOC in the presence of disorder have been previously considered, see e.g. Ref. 15. In the present paper we try to circumvent the task of analyzing the AOC in the presence of disorder potential, and replace this challenge by studying the AOC within the framework RMT. Here the role of an added perturbation is played by a parameter which is varied. We end up studying the AOC in the context of parametric random matrices<sup>16</sup>. As has been argued recently<sup>17</sup> this is a good model to describe electron scrambling in quantum dots embedding the discrete electron number in the dot in a continuous variation of a parameter.<sup>13</sup>

The paper is organized as follows. In Section II we rederive the expression for the ground state overlaps, reviewing the main features of the theory and introducing the notation employed throughout this work. Section III is devoted to the presentation of the random matrix model used in this study. Section IV contains the main body of our analysis, presenting our analytical and numerical results for the *averaged* ground state overlaps. The distribution of  $|S|$  is the subject of Section V. Section VI contains some brief concluding remarks. We have also included three appendices. Appendix A quantifies the accuracy of the “unit volume approximation” used by Anderson in his original work<sup>1</sup>. In Appendix B we discuss some implications of evaluating the ensemble-averaged value of the Anderson integral subject to *grand canonical* constraints. Finally in Appendix C we discuss the precision of the first order perturbation theory used to evaluate Anderson's integral, defined in Section II.

## II. REMINDER ON THE ANDERSON ORTHOGONALITY CATASTROPHE: A PARAMETRIC APPROACH

Let us consider systems of electrons whose Hamiltonian,  $H(X)$  is a function of a parameter  $X$ . In this study the generic parameter  $X$  can be either continuous or discrete. In the case of modelling the change in an external magnetic field or in the electrostatic potential,  $X$  is continuous. One can also imagine  $X$  as modelling the change in the *effective* single-particle potential due to the sequential addition of electrons to the system, in which case  $X$  is discrete (in the latter case it is necessary first to subtract all systematic changes of the single-particle spectrum.) It has been shown recently<sup>18</sup> that scrambling due to the sequential addition of electrons to the QD can be embedded in a parametric RM process only if interaction matrix elements due to the accumulation of surface charge are taken into account. The subject of the present paper is the overlap  $S$  between ground states of systems corresponding to  $H(X)$  and  $H(X + \delta X)$ . In particular, this section is devoted to the presentation of different levels of approximation for  $\log |S|$ .

Since we are dealing with non-interacting electrons, the ground state wave functions are Slater determinants. The overlap  $S$  can then be expressed in terms of the occupied single-particle wave functions overlap. Let us denote by  $\psi_k(X)$  and  $\psi_k(X + \delta X)$  the (single-particle) eigenstates of  $H(X)$  and  $H(X + \delta X)$  respectively. We define the unitary overlap matrix  $A$  as

$$A_{ij} = \langle \psi_i(X) | \psi_j(X + \delta X) \rangle. \quad (5)$$

Thus the overlap of the ground states  $S$  can be written as

$$S = \det A^{oo}, \quad (6)$$

where the superscript “o” stands for occupied states. Accordingly  $A^{\text{oo}}$  corresponds to the subspace of occupied states of the matrix  $A$  defined in Eq. (5).

The catastrophe is manifest by the fast suppression of the overlap  $S$  as the number of fermions  $n$  in the system is increased for a fixed perturbation strength. Anderson<sup>1</sup> singled out two basic reasons that make the absolute value of the overlap  $S$  smaller than one: The rows of  $A^{\text{oo}}$  have norms smaller than unit and they do not form an orthogonal set. It is convenient to separate these two contributions by introducing a new matrix  $\widetilde{A}^{\text{oo}}$  with normalized rows, defined as

$$\left(\widetilde{A}^{\text{oo}}\right)_{ij} = (A^{\text{oo}})_{ij} / \mathcal{N}_i, \quad (7)$$

where the normalization factor  $\mathcal{N}_i$  reads

$$\mathcal{N}_i = \sqrt{\sum_{j=1}^n [(A^{\text{oo}})_{ij}]^2}. \quad (8)$$

$|S|$  is then rewritten as

$$|S| = |\det \widetilde{A}^{\text{oo}}| \times \prod_{i=1}^n \mathcal{N}_i. \quad (9)$$

The absolute value of  $\det \widetilde{A}^{\text{oo}}$  can be geometrically interpreted as the volume of a  $n$ -dimensional parallelepiped defined by a set of non-orthogonal vectors of unit length. In Ref. 1 it is claimed that  $|\det \widetilde{A}^{\text{oo}}|$  does not depend on  $n$  and it is close to one. In Appendix A we show perturbatively that indeed the most important contributions to  $|S|$  come from  $\prod \mathcal{N}_i$ , the deviations from the “unit volume approximation” being of higher order in  $\delta X$ . Aiming at obtaining an upper bound of the overlap  $S$  we shall neglect below the contribution of  $|\det \widetilde{A}^{\text{oo}}|$  to  $|S|$ . We thus restrict our analysis to the product of normalization factors. We can therefore write

$$|S| < \prod_{i=1}^n \mathcal{N}_i \equiv \prod_{i=1}^n (1 - P_i)^{1/2}, \quad (10)$$

where we have introduced

$$P_i = \sum_{j=n+1}^{\infty} |\langle \psi_i(X) | \psi_j(X + \delta X) \rangle|^2. \quad (11)$$

$P_i$  measures the probability of the state  $i$ , whose energy  $\varepsilon_i$  is smaller than the Fermi energy, to be spread over the  $j$ -components lying above the Fermi surface once the Hamiltonian is changed. The product of the normalization factors, Eq. (10), is the first level of approximation to the overlap determinant considered here. For the sake of convenience, hereafter we shall deal with  $\log |S|$  instead of  $|S|$  itself, and define

$$I_{\text{norm}} \equiv \frac{1}{2} \sum_{i=1}^n \log(1 - P_i) > \log |S|. \quad (12)$$

Eq. (12) is still not suitable for an insightful analysis. For this purpose a higher level of approximation for  $S$  was introduced<sup>1</sup>. For small  $\delta X$  the “probabilities”  $P_i$  will also be small. Thus, by expanding  $I_{\text{norm}}$  in a power series

$$I_{\text{norm}} = \frac{1}{2} \sum_{i=1}^n \left( -P_i - \frac{P_i^2}{2} - \dots \right) \quad (13)$$

and retaining only its first expansion term one writes

$$I \equiv -\frac{1}{2} \sum_{i=1}^n P_i > I_{\text{norm}}. \quad (14)$$

By explicitly expressing  $I$  in terms of the single-particle overlaps, one arrives at

$$I = -\frac{1}{2} \sum_{i=1}^n \sum_{j=n+1}^{\infty} |\langle \psi_i(X) | \psi_j(X + \delta X) \rangle|^2. \quad (15)$$

This is the well known *Anderson integral* term. The approximations  $I_{\text{norm}}$  and  $I$  for  $\log |S|$  will be analyzed at length in Section IV where we present numerical and analytical results for the random matrix model introduced in the forthcoming section.

### III. THE RANDOM MATRIX MODEL

In this Section we present a model for the statistical study of the Anderson orthogonality catastrophe in ballistic ergodic systems. The setting is the same as in the foregoing Section. We model the single-particle Hamiltonian  $H$  which depends on a parameter  $X$  by a suitable ensemble of random matrices. In one of its simplest forms<sup>19</sup>, such model is realized by

$$H(X) = H_0 \cos X + U \sin X, \quad (16)$$

where  $H_0$  and  $U$  are two independent matrices of dimension  $N \times N$ , both members of the same Gaussian Ensemble. In this study, we restrict our analysis to the Gaussian Orthogonal Ensemble ( $\beta = 1$ ) and to the Gaussian Unitary Ensemble ( $\beta = 2$ ). Whereas the orthogonal ensemble is used to model systems presenting time-reversal symmetry, the unitary ensemble models systems where the latter symmetry is absent. Thus the distribution of  $H_0$  and  $U$  is<sup>6,7</sup>

$$P(H_0, U) = C_{\beta N} \exp \left\{ -\frac{2N}{\beta \lambda^2} (\text{tr } H_0 H_0^\dagger + \text{tr } U U^\dagger) \right\}, \quad (17)$$

where  $C_{\beta N}$  is a normalization constant. As a consequence of this choice, the matrix elements of  $H(X)$  are

also Gaussian distributed with zero mean and variance parameterized as

$$\langle H_{ij}^*(X) H_{i'j'}(X) \rangle = (\delta_{ii'} \delta_{jj'} + \delta_{\beta 1} \delta_{ij'} \delta_{ji'}) \frac{\lambda^2}{N} \quad (18)$$

independent of  $X$ . Here the symbols  $\langle \dots \rangle$  stand for ensemble averaging.

For any arbitrary value of  $X$ , the resulting mean level density is given by the well-known Wigner semicircle formula<sup>6</sup>

$$\rho(\varepsilon) = \frac{N}{\pi\lambda} \sqrt{1 - \left(\frac{\varepsilon}{2\lambda}\right)^2}, \quad (19)$$

where  $\varepsilon$  is the single-particle energy. Evidently, the mean level spacing at the center of the spectrum ( $\varepsilon = 0$ ) is  $\Delta = \pi\lambda/N$ . Accordingly, the average band width is  $\varepsilon_{\max} - \varepsilon_{\min} = 4\lambda$  (this is in line with standard solid state picture whereby the band width is fixed, independent of the system's size, while the mean level spacing scales as  $N^{-1}$ ).

The typical scale for the parametric variation  $X^*$  representing the average distance between anticrossings, can in general be characterized by the level velocity standard deviation<sup>20,21</sup>

$$\frac{\Delta}{X^*} = \sqrt{\left\langle \left( \frac{d\varepsilon_\mu}{dX} \right)^2 \right\rangle - \left\langle \frac{d\varepsilon_\mu}{dX} \right\rangle^2}, \quad (20)$$

where  $\varepsilon_\mu(X)$  is an energy level of  $H(X)$  close to the center of the band. In the model defined by Eqs. (16) and (17) the average level velocity is zero and

$$X^* = \frac{\Delta}{\sqrt{2/(\beta N)} \lambda} = \pi \sqrt{\frac{\beta}{2N}}. \quad (21)$$

Now it is possible to quantify the effect of  $\delta X$  in the single-particle spectrum by the scaled parameter  $x \equiv \delta X/X^*$ .

It remains to specify the many-body part of the model. The ground state configuration is generated by populating the single-particle levels with  $n = N/2$  fermions (the spin degree of freedom is not considered here). For a given  $X$ , the ground state is the Slater determinant made up of the lowest  $N/2$  eigenstates of  $H(X)$ . Now the single particle Hilbert space is finite and of size  $N$ , and the number of particles is  $N/2$ . The Fermi level,  $\varepsilon_F = (\varepsilon_{N/2+1} + \varepsilon_{N/2})/2$ , lies on average at  $\varepsilon_F = 0$ . It is important to stress that the sums in Eqs. (11) and (15) have to be modified accordingly.

Numerical simulations of the model presented above are straightforward to implement. We generate a pair of matrices  $H_0$  and  $U$  of dimension  $N$  whose elements are Gaussian distributed with zero mean and variance given by Eq. (18). Fixing  $X$  and  $x$  we calculate the eigenvalues and eigenfunctions of the corresponding  $H(X)$  and  $H(X + \delta X)$ . Having computed the complete set of eigenfunctions, we calculate the overlap matrix  $A^{\circ\circ}$  and its

determinant,  $S_N(X, x)$ . In order to keep the notation simple, we shall write down the arguments of  $S$  explicitly only when necessary.

As a guide for the discussions to come let us consider a representative member of the ensemble defined by Eq. (17) for  $\beta = 1$  and  $N = 50$ . In Fig. 1 we show the parametric spectrum as a function of  $X$  around  $\varepsilon = 0$  (top panel) and the corresponding ground state overlaps  $|S(X)|$  for  $x = 0.4$  (bottom panel), both obtained by a direct numerical procedure. The most striking feature of this plot is that large fluctuations in  $|S|$  are closely correlated with the occurrence of narrow avoided crossings at the Fermi surface. In other words, to each narrow gap (avoided crossing) there corresponds a small overlap  $|S|$ .

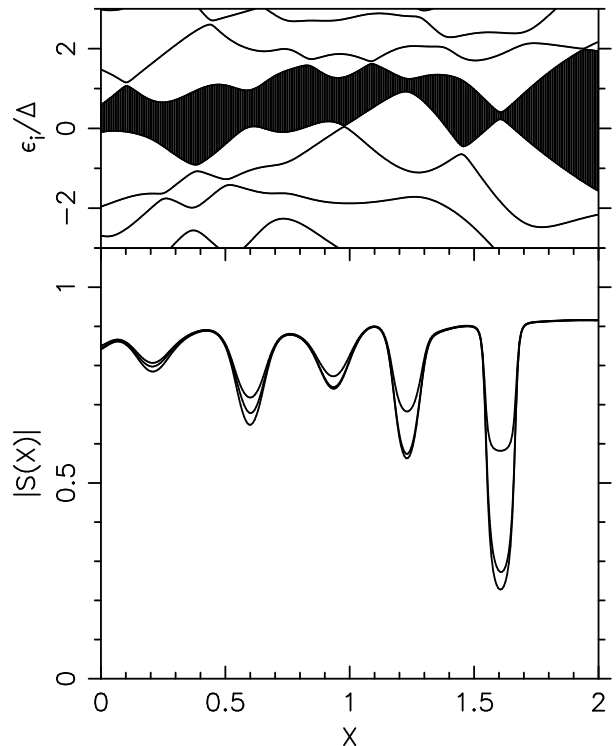


FIG. 1. Top panel: typical energy levels as a function of  $X$ . The filled region is the gap between the last occupied and the first empty single-particle levels. Bottom: the three curves represent the exact overlap  $S$ ,  $\exp(I_{\text{norm}})$ , and  $\exp(I)$  (see text for definitions) as a function of  $X$ . They respect the ordering  $S < \exp(I_{\text{norm}}) < \exp(I)$ . The parametrical distance is set to  $x = 0.4$  ( $\delta X \approx 0.13$ ) and the dimension of the single particle Hilbert space is  $N = 50$ .

The figure also suggests that the approximation schemes presented in Section II fail in the vicinity of narrow gaps. These observations indicate that an accurate analytical estimate of the average  $|S|$  and its variance requires a good handle of the “two-level problem” of narrow avoided crossings. Had we considered integrable (or mixed) systems, this issue would become even more important due to the absence (or suppression) of level repulsion.

#### IV. AVERAGE GROUND STATES OVERLAP

As we shall argue in the next section, the distribution of  $S$  can be anomalously broad. As a first step though, we shall consider in this section *ensemble averaged* quantities. When the distribution is narrow, as is often the case with thermodynamic quantities, one may interchange

$$\langle \log |S| \rangle \approx \log \langle |S| \rangle. \quad (22)$$

Evidently, when in doubt, the meaningful quantity is the r.h.s. of the equation above. Technically, though, the more accessible quantity is the l.h.s. of Eq. (22). This section is devoted to the statistical study of upper bounds for  $\langle \log |S| \rangle$  within the approximation levels presented in Section II and the random matrix model described in Section III. Our analytical results are complemented with numerical simulations.

In Eq. (15) the ground states overlap can be easily evaluated by considering the single-particle overlaps in first order perturbation theory, namely

$$\langle \psi_i(X) | \psi_j(X + \delta X) \rangle \approx \frac{\delta H_{ij}}{\varepsilon_j - \varepsilon_i}. \quad (23)$$

Here  $\delta H \approx (-H_0 \sin X + U \cos X) \delta X$  and  $\{\varepsilon_j\}$  are the eigenvalues of  $H(X)$ . The matrix  $\delta H$  and the set of eigenvalues  $\{\varepsilon_j\}$  are statistically independent due to the invariance of the considered ensembles under orthogonal ( $\beta = 1$ ) or unitary ( $\beta = 2$ ) transformations. Recalling Eq. (15)  $\langle \log |S| \rangle$  now reads

$$\langle \log |S| \rangle < \langle \tilde{I} \rangle \equiv -\frac{1}{2} \sum_{i=1}^{N/2} \sum_{j=N/2+1}^N \left\langle \frac{|\delta H_{ij}|^2}{(\varepsilon_j - \varepsilon_i)^2} \right\rangle. \quad (24)$$

In Appendix A it is shown that the corrections responsible for the inequality in Eq. (24) are of fourth order in a perturbation expansion. Note that only off-diagonal  $\delta H_{ij}$  matrix elements contribute in Eq. (23) since the  $i$ -states lie below the Fermi surface and the label  $j$  corresponds to states above it. The ensemble average over  $|\delta H_{ij}|^2$ , defined in Eq. (18), yields

$$\langle \tilde{I} \rangle = -\frac{1}{2} \sum_{i=1}^{N/2} \sum_{j=N/2+1}^N \frac{\beta}{2} x^2 \left\langle \frac{\Delta^2}{(\varepsilon_j - \varepsilon_i)^2} \right\rangle, \quad (25)$$

where we have used  $X^*$  of Eq. (21) to express  $\langle \log |S| \rangle$  in terms of the dimensionless variable  $x = \delta X / X^*$ .

A satisfactory accuracy of the approximation introduced by Eq. (23) requires  $\delta H_{ij} / (\varepsilon_j - \varepsilon_i)$  to be small. Such a condition is translated to  $\langle \tilde{I} \rangle$  by examining separately  $x^2$  and  $\langle \Delta^2 / (\varepsilon_j - \varepsilon_i)^2 \rangle$ . Viewed from the perspective of the parametric framework, the approximation is under control since the physical situations in mind, see Section I, call for  $x \ll 1$ , or at least for  $x < 1^2$ . By contrast, the average over  $\Delta^2 / (\varepsilon_j - \varepsilon_i)^2$  requires a careful discussion.

The occurrence of small gaps at the Fermi surface,  $\varepsilon_j - \varepsilon_i \ll \Delta$  for  $j - i = 1$ , causes the breakdown of the perturbation approach employed in Eq. (23), to calculate  $\langle \psi_i(X) | \psi_{i+1}(X + \delta X) \rangle$ . In that case even a small variation of  $x \ll 1$  may give rise to a significant mixing of an originally occupied level (the last one) and an empty one (the lowest original vacant level). Such a situation calls for a non-perturbative solution. Indeed it is tempting to justify the approximation used in Eq. (23) invoking the presence of level repulsion: the large errors introduced in the calculation of  $|S|$  at small gaps are minimized by the rareness of such events. Unfortunately, such a scheme is doomed to fail due to the following reason: For neighboring levels

$$\left\langle \frac{\Delta^2}{(\varepsilon_{i+1} - \varepsilon_i)^2} \right\rangle = \int_0^\infty ds s^{-2} P_\beta(s), \quad (26)$$

where  $P_\beta(s)$  is the nearest neighbor spacing distribution<sup>6</sup>. Since,  $P_\beta(s) \sim s^\beta$  for  $s \ll 1$  the average on the l.h.s. of Eq. (26) diverges for the orthogonal symmetry (although not for the unitary case). This motivates the employment of a non-perturbative approach to account for the effect of the “crust levels” (near the Fermi energy) on the ensemble-averaged Anderson integral. With this proviso in mind it should be also realized that  $j - i = 1$  corresponds to a single term in the double sum of Eq. (25). As concluded from Fig. 1 this term has a *major contribution to the large fluctuations* in  $|S|$  and will be the subject of analysis of Section V. By now it is only necessary to anticipate that the occurrence of narrow gaps contributes to  $\langle \log |S| \rangle$  with an additional factor which depends on  $x$  and on the size of the narrow gap. Note that the procedure presented in Eq. (26) represents averaging under *canonical* conditions, namely averaging over systems with a given particle number  $N^{22}$  or averaging over both impurity realizations and  $N$ . Such procedures are referred to as strong and weak canonical averaging, cf. Ref. 23. There are experimental setups where it is the chemical potential,  $\mu$ , which is the controlled parameter. In such circumstances it is more appropriate to employ a grand-canonical averaging procedure. This is briefly discussed in Appendix B.

As the value of  $j - i$  becomes larger the perturbative approach works increasingly better. Moreover, at the same time the fluctuations of  $\varepsilon_j - \varepsilon_i$  relative to  $(j - i)\Delta$  decrease as a consequence of the spectral rigidity. These matters are discussed in Appendix C. In this regime we do not expect to introduce a large error (independent of  $N$ ) replacing the spectrum of  $H(X)$  by its average spectrum, that is

$$\left\langle \frac{1}{(\varepsilon_j - \varepsilon_i)^2} \right\rangle \approx \frac{1}{(\langle \varepsilon_j \rangle - \langle \varepsilon_i \rangle)^2}. \quad (27)$$

The latter approximation allows us write

$$\langle \tilde{I} \rangle = -\frac{\beta}{4} x^2 \int_{-2\lambda}^{-\Delta/2} d\varepsilon_i \int_{\Delta/2}^{2\lambda} d\varepsilon_j \frac{\rho(\varepsilon_i) \rho(\varepsilon_j)}{(\varepsilon_j - \varepsilon_i)^2}, \quad (28)$$

with the mean level density  $\rho(\varepsilon)$  given by the Wigner semicircle law, Eq. (19). Changing variables and defining  $\alpha \equiv \pi/(4N)$  we arrive at

$$\langle \tilde{I} \rangle = -\frac{\beta}{4} x^2 \int_{\alpha}^1 du \int_{\alpha}^1 dv \frac{\sqrt{1-u^2} \sqrt{1-v^2}}{(u+v)^2}. \quad (29)$$

We can now isolate the singularity at  $\alpha = 0$  ( $N$  large) and rewrite the integral on the r.h.s. of Eq. (29)

$$\int_{\alpha}^1 du \int_{\alpha}^1 dv \left[ \frac{1}{(u+v)^2} + \frac{\sqrt{1-u^2} \sqrt{1-v^2} - 1}{(u+v)^2} \right]. \quad (30)$$

While it is the first term under the integral in Eq. (30) which is ultimately responsible for the catastrophe, the second one gives only a constant as  $\alpha \rightarrow 0$ . The final result is therefore

$$\langle \tilde{I} \rangle = -\frac{\beta}{4} x^2 (\log N + C), \quad (31)$$

where  $C = -\log(\pi/2) - \pi^2/8$ . The latter constant has to be taken with caution due to the approximations made.

Summarizing our results, we have several levels of approximation to the exact value of  $\langle \log |S| \rangle$ . The product of the normalization factors, which neglects corrections to the volume of the parallelepiped, assumed to be unity, yields

$$\langle \log |S| \rangle \approx \langle I_{\text{norm}} \rangle \equiv \frac{1}{2} \sum_{i=1}^{N/2} \langle \log(1 - P_i) \rangle. \quad (32)$$

By keeping only the first term of the expansion of the logarithm in  $I_{\text{norm}}$  we have

$$\langle \log |S| \rangle \approx \langle I \rangle \equiv -\frac{1}{2} \sum_{i=1}^{N/2} \langle P_i \rangle. \quad (33)$$

By calculating  $I$  using first order perturbation theory and a smoothed spectrum, we obtain the analytical estimate  $\langle \tilde{I} \rangle$ , given by Eq. (31).

For small values of  $x$  these quantities are close to each other. They are ordered as follows:

$$\langle \log |S| \rangle < \langle I_{\text{norm}} \rangle < \langle I \rangle < \langle \tilde{I} \rangle. \quad (34)$$

We turn now to our numerical analysis. For different values of  $x$  and  $N$  we have evaluated  $\langle \log |S| \rangle$ ,  $\langle I_{\text{norm}} \rangle$ ,  $\langle I \rangle$ , and  $\langle \tilde{I} \rangle$  ensemble averaging over  $M$  realizations of  $H(X)$  which is defined in Section III. Each simulation is performed at the cost of the order of  $M \times (\beta \times N)^3$  operations, imposing a computational constraint on the procedure.

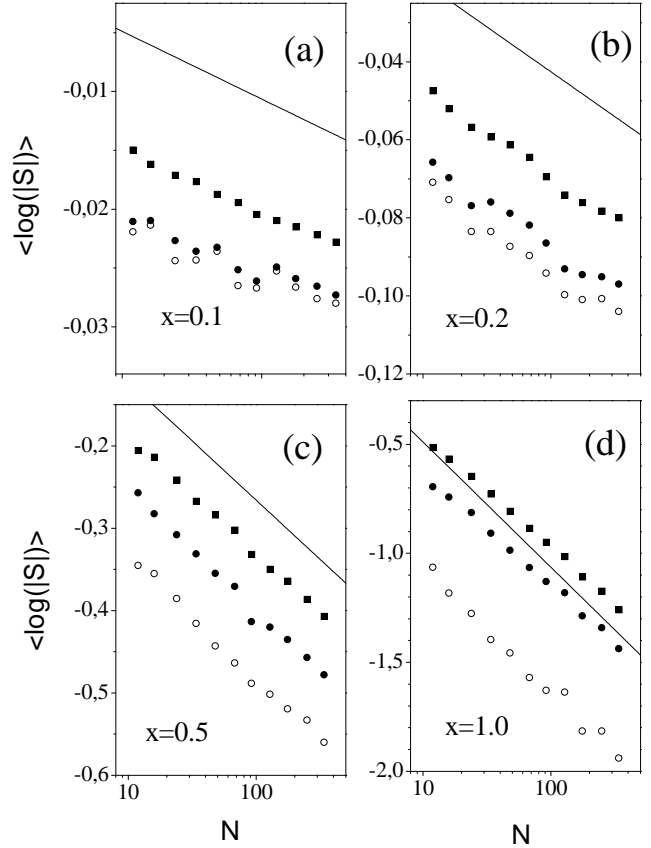


FIG. 2. The average  $\log |S(x)|$  as a function of  $N$ . The number of realizations for each  $N$  is  $M = 10^4$  and (a)  $x = 0.1$ , (b)  $x = 0.2$ , (c)  $x = 0.5$ , and (d)  $x = 1.0$ . Open dots stand for the exact  $\langle \log |S| \rangle$ , filled dots for  $\langle I_{\text{norm}} \rangle$ , squares for  $\langle I \rangle$ , whereas the solid lines represent  $\langle \tilde{I} \rangle$ .

In Fig. 2 we show a comparison between the different approximations for  $\langle \log |S| \rangle$  as a function of  $N$  for  $\beta = 1$ . We chose four representative values of  $x$  and fixed  $M = 10^4$ . We observe that in all approximation schemes  $\langle \log |S| \rangle$  displays the slope predicted by Eq. (31). In view of the large sample sizes, the fluctuations in the mean values indicate the corresponding distributions are characterized by large standard deviations, as we discuss in the following section. As analyzed in Appendix C the first order perturbation theory estimate breaks down when used for levels in the vicinity of the Fermi surface and/or for not sufficiently small values of  $x$ . As the latter is increased we even expect deviations from the predicted slopes for  $\langle I \rangle$  versus  $\log N$ . In Fig. 2 such discrepancies are only noticeable for  $x = 1$  at  $N \leq 50$ . We conclude that the power law suppression of  $|S|$  as a function of  $N$  is very robust. The discussion presented in Appendix C suggests why our theoretical estimate does not always serve as an upper bound for all our approximation schemes. This is done by noting two facts. (i) For small values of  $x$  the perturbation approach underestimates  $\langle |A_{N/2, N/2+j}|^2 \rangle$ , hence overestimates the overlap. In such cases we are guaranteed an upper bound. (ii)

For larger values of  $x$  the situation is quite the opposite. When this happens the constant  $C$  does not provide any longer an upper bound. Results for the  $\beta = 2$  case behave in the very same way as for  $\beta = 1$ , with slopes following Eq. (31). (We have thus decided to omit a corresponding figure for the unitary case).

Figure 2 also confirms Anderson's claim that the "unit volume" corrections to  $\langle \log |S| \rangle$  are small, at least for  $x \ll 1$ , as indeed is seen in panels (a) and (b). While within our statistical precision we do not observe any  $N$  dependence for the unit volume corrections, the latter cannot be ruled out.

## V. DISTRIBUTION OF OVERLAPS AND THEIR LARGE FLUCTUATIONS

This section is devoted to the analysis of the distribution of the overlaps between ground states,  $P(|S|)$ . We show that the large fluctuations of  $S(X)$  occurring in the vicinity of small gaps at the Fermi surface are well described by a  $2 \times 2$  model, otherwise  $\exp(\langle \tilde{I} \rangle)$  provides a satisfactory estimate for  $|S|$ .

Let us start quantifying the influence of the narrow avoided crossings on the overlap determinant. In the proximity of a narrow gap the single-particle overlap  $\langle \psi_{N/2}(X) | \psi_{N/2}(X + \delta X) \rangle$  will be small and rapidly varying with  $X$ . Consequently, as it was qualitatively established in Section II, it will dominate the fluctuations of the single-particle overlap matrix determinant. In this situation we expect that the behavior of  $S$  will be captured by the approximation

$$|S_N(X, \delta X)| \approx K_N(X, \delta X) |\langle \psi_{N/2}(X) | \psi_{N/2}(X + \delta X) \rangle|. \quad (35)$$

This approximation is just the first term of the expansion of the determinant of  $A^{\circ\circ}$  along its  $N/2$ -th row. In other words, we calculate  $|S|$  as if all fluctuations are due to the interaction of the highest occupied single-particle level with the lowest empty one. The factor  $K$  accounts for the contribution of all remaining states and will be approximately constant:

$$K_N(X, \delta X) \approx \langle |S_{N-1}(X, \delta X)| \rangle. \quad (36)$$

The results presented in Fig. 3 confirm that this approximation works impressively well *in the vicinity of narrow gaps* and for small values of  $x$ . The system is the same as that in Fig. 1, but smaller deformation is considered,  $x = 0.2$ , as well as a smaller parameter range for  $X$ . The latter contains, in the present example, two narrow gaps (cf. Fig. 1). The small shift between the two curves can be attributed to the  $K$  term. The proposed approximation gives rise to spurious peaks whenever an avoided crossing (narrow gap) between the occupied levels  $N/2$  and  $N/2 - 1$  is encountered. Such cases are beyond the

scope of our approximation: the factorization put forward by Eq. (35) is no longer valid, and the gap at the Fermi energy is certainly not small. The spurious peak at  $X \approx 1.45$  in Fig. 3 represents such a situation, as can be verified from Fig. 1.

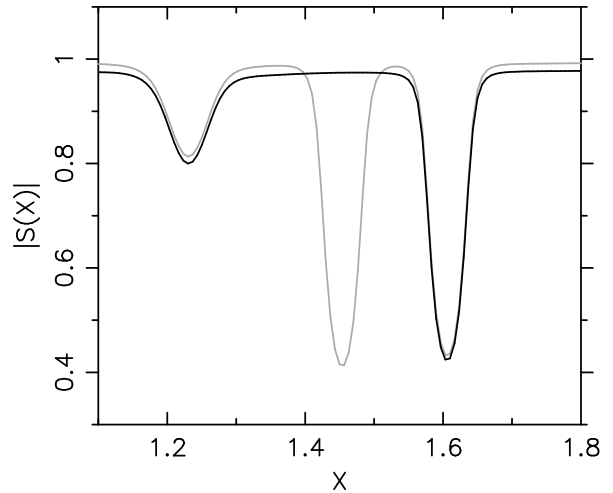


FIG. 3. Overlaps of Slater determinants for  $x = 0.2$  as a function of  $X$  for  $N = 50$ . The exact determinant is shown as a black line. The grey line corresponds to the approximation  $|S| \approx |\langle \psi_{N/2}(X) | \psi_{N/2}(X + \delta X) \rangle|$ .

We have thus demonstrated heuristically that small Anderson overlaps arise due avoided crossings at the Fermi level, involving the highest occupied and the lowest unoccupied levels. This observation leads us to conjecture that

$$P(|S|) \approx P(K \cdot |\tilde{S}|) \quad \text{for} \quad |S| \ll 1, \quad (37)$$

where  $\tilde{S} = \langle \psi_{N/2}(X) | \psi_{N/2}(X + \delta X) \rangle$ . The derivation of an expression for  $P(|\tilde{S}|)$ , which calls for a non-perturbative approach, is discussed now. Due to level repulsion two levels rarely come very close to each other. When this happens, it is possible to effectively model a narrow avoided crossing by a  $2 \times 2$  matrix, since it is quite unlikely to have yet another level very close by. This model also rids of the undesired occurrence of spurious peaks as the one shown by Fig. 3: they cancel between the factor  $K$  and  $\tilde{S}$ . While this is quite a simple model, the calculation of the distribution  $P(|\tilde{S}|)$  involves some cumbersome multidimensional integrals<sup>24</sup>.

For the orthogonal case,  $\beta = 1$ , the integrations can be simplified through a geometrical construct, which makes it possible to obtain  $P(|\tilde{S}|)$  analytically within a  $2 \times 2$  parametric random matrix model. Let us write our model Hamiltonian, Eq. (16),  $H(X) = H_0 \cos X + U \sin X$  as

$$H(X) = \cos X (H_0 + U \tan X). \quad (38)$$

Let us also parameterize its eigenvector as  $\psi = (\cos \theta, \sin \theta)$ . Then, by defining the vector  $\mathbf{h}(X) \equiv$

$(2H_{12}, H_{22} - H_{11})$ , it is straightforward to show that the eigenvector equation can be written as

$$(2H_{12}, H_{22} - H_{11}) \cdot (\cos 2\theta, \sin 2\theta) = 0, \quad (39)$$

so that the eigenvectors are determined solely by the vector  $\mathbf{h}(X)$ . Moreover, the angle between  $\psi(X + \delta X)$  and  $\psi(X)$  is half the angle  $\alpha$  between  $\mathbf{h}(X + \delta X)$  and  $\mathbf{h}(X)$ , that is  $|S| = \cos \alpha/2$ . Now the problem is reduced to finding the distribution of  $\alpha$ . Let us set  $X = 0$  and introduce

$$\begin{aligned} \mathbf{h}(X=0) &\equiv \mathbf{h}_0 = (2[H_0]_{12}, [H_0]_{22} - [H_0]_{11}) \\ \mathbf{h}(\delta X) &\equiv \mathbf{h}_t = (2[H_0]_{12}, [H_0]_{22} - [H_0]_{11}) + \\ &\quad (2U_{12}, U_{22} - U_{11})t, \end{aligned} \quad (40)$$

with  $t = \tan \delta X$ . The usefulness of this geometrical construction becomes clear now. We use the fact that  $\mathbf{h}_t = \mathbf{h}_0 + \mathbf{u}t$  and

$$\mathbf{h}_t \cdot \mathbf{h}_0 = |\mathbf{h}_t| |\mathbf{h}_0| \cos \alpha, \quad (41)$$

where the vectors  $\mathbf{h}_t$  and  $\mathbf{h}_0$  can be expressed in terms of  $|h_0|$ ,  $|u|$ ,  $\theta_u$ , and  $\alpha$ . The integration of  $P(\mathbf{h}_0, \mathbf{h}_t)$  over  $\mathbf{h}_0, u$  and  $\theta_u$ , readily gives  $P(\alpha)$ .

The distribution  $P(\mathbf{h}_0, \mathbf{h}_t)$  is written in terms of  $H_0$  and  $U$  matrix elements, Eq. (17), as

$$P(\mathbf{h}_0, \mathbf{h}_t) = t^2 P\left(\mathbf{h}_0, \mathbf{u} = \frac{1}{t}[\mathbf{h}_t - \mathbf{h}_0]\right). \quad (42)$$

The integration over the vectors  $\mathbf{h}_0$  and  $\mathbf{h}_t$ , keeping their relative orientation fixed, yields

$$P(\alpha) = \frac{2t^2}{\pi} \int_0^{\pi/2} d\phi \frac{\cos \phi \sin \phi}{(1 + t^2 \cos^2 \phi - 2 \cos \phi \sin \phi \cos \alpha)^2}. \quad (43)$$

The latter is expressed in a closed form as

$$P(\alpha) = \frac{t^2}{\pi (\sin^2 \alpha + t^2)} [1 + G(\alpha)], \quad (44)$$

with

$$G(\alpha) = \frac{\cos \alpha}{\sqrt{\sin^2 \alpha + t^2}} \left[ \frac{\pi}{2} + \tan^{-1} \left( \frac{\cos \alpha}{\sqrt{\sin^2 \alpha + t^2}} \right) \right]. \quad (45)$$

Since we are not really interested in  $P(\alpha)$ , but rather in  $P(|\tilde{S}|)$  instead, a last change of variables is needed to arrive at the main result of this section

$$P(|\tilde{S}|) = 2 \frac{P[\alpha = 2 \cos^{-1} |\tilde{S}|]}{\sqrt{1 - |\tilde{S}|^2}}. \quad (46)$$

In particular, the probability density of having a null overlap is non-vanishing and is given by

$$P(|\tilde{S}| = 0) = \frac{2}{\pi} \left( 1 - \frac{\delta X}{\tan \delta X} \right). \quad (47)$$

Comparison between the analytic form of  $P(K \cdot |\tilde{S}|)$ , Eq. (46) [cf. also Eq. (37)], and our numerical study of the exact distribution of overlaps  $P(|S|)$  is displayed in Fig. 4. It is evident that the 2-level picture reproduces the tails of the distributions  $P(|S|)$  for large  $N$  remarkably well, provided we use the same relative deformation  $x$ . Note that for  $N = 2$  and  $\beta = 1$ , one has  $X^* = \sqrt{\pi}$ , differing from the large  $N$  limit given by Eq. (21), see for instance Ref. 25. The correction due to  $K_N$ , a rescaling of the horizontal axis, is negligible in this case (from Fig. 3 one finds that  $K \approx 0.98$ ) and was not included.

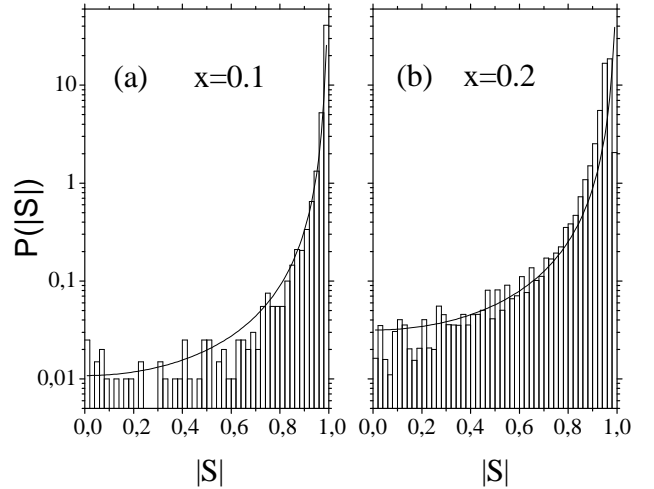


FIG. 4. Log-normal plot of the distribution of overlaps  $P(|S|)$ . We compare the analytical prediction based on the case  $N = 2$  with numerical simulations over  $10^5$  pairs  $(H_0, U)$  (histograms), for  $N = 100$ . The relative deformation is (a)  $x = 0.1$  and (b)  $x = 0.2$ .

The agreement between the output of our  $2 \times 2$  model and the exact diagonalization becomes even more evident by analyzing the cumulative overlap distribution in a log-log plot, as is seen from Fig. 5



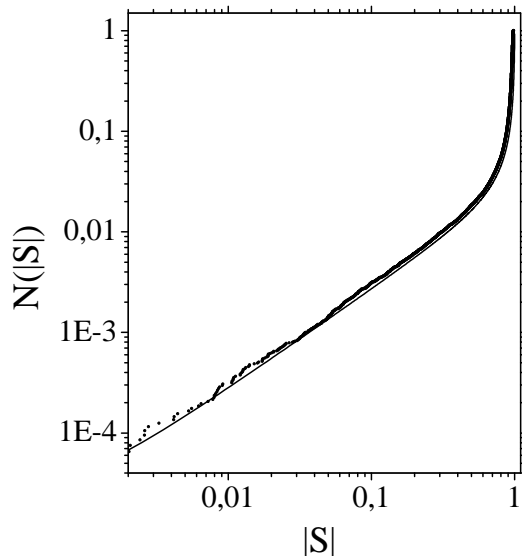


FIG. 5. Log-log plot of the cumulative distribution of overlaps  $N(|S|) = \int_0^{|S|} d|S| P(|S|)$ . We compare (i) the analytical prediction based on the case  $N = 2$  and (ii) numerical simulations over  $10^5$  pairs  $(H_0, U)$  (dots), for  $N = 50$ . In both cases the relative deformation is  $x = 0.2$ .

## VI. CONCLUDING REMARKS

We have studied the orthogonality catastrophe due to a parametric change of the single-particle of an ergodic system. The Hamiltonian was modelled by a suitable random matrix ensemble. We show that the average overlap between the original and the parametrically modified many-body ground states, taken as Slater determinants, decreases like  $n^{-\beta x^2/4}$ , where  $n$  is the number of electrons in the system and  $x$  is the deformation measured in units of the typical distance between anticrossings. We have also shown that the fluctuations of  $\log |S|$  are enormous. To account for the latter in the orthogonal case ( $\beta = 1$ ), we have put forward a simple  $2 \times 2$  matrix model and employed it to obtain a prediction for  $P(|S|)$  for  $|S| \ll 1$ , in good agreement with our numerical analysis. In the unitary case ( $\beta = 2$ ) the fluctuations are smaller, but still quite significant. Here also it was shown<sup>24</sup> that the  $2 \times 2$  model works well, but no simple analytical expression is available.

This model study constitutes a first step towards understanding the relevance of the orthogonality catastrophe for ballistic ergodic systems. One improvement to the theory presented in Section IV should arise from the fact that for a generic dynamical system the “perturbation” matrix,  $\delta H_{ij}$ , will in general have a finite bandwidth  $b$ . How are our results changed in this case? There is extensive literature dealing with the matrix elements properties of low-dimensional dynamical systems. In particular, for the case of a two-dimensional chaotic ballistic system, the bandwidth for a “generic” perturbation was

estimated<sup>27,28</sup> to be

$$b = \frac{\hbar^2}{\tau \Delta}, \quad (48)$$

where  $\tau$  is a time needed for a particle to traverse the system, i.e.,

$$\tau \approx \frac{L}{v_F}. \quad (49)$$

Here  $L$  is the linear dimension of the system and  $v_F$  is the Fermi velocity. Relating the 2D mean level spacing to the system’s size,  $\Delta = 2\pi\hbar^2/(mL^2)$ , and using  $\varepsilon_F \approx n\Delta$ , we obtain a simple relation between the bandwidth and the number of electrons, namely,  $b \approx \sqrt{n}$ . In line with the present study, we assume that within the band  $|j-i| < b$ , the fluctuations of  $\delta H_{ij}$  are statistically well described by RMT. Accordingly, the average of  $\log |S|$ , obtained in Eqs. (32), (33), becomes

$$\langle \log |S| \rangle \approx -\frac{\beta}{4} x^2 \log \sqrt{n}. \quad (50)$$

We stress that in order to write Eq. (50), two important assumptions have been made. (i) The Hamiltonian  $H(X)$  must be fully chaotic.<sup>27</sup> (ii) The perturbation must be generic in the sense defined in Ref. 28. If such conditions are not met, the statistical distribution of  $\delta H_{ij}$  could strongly depend on  $|j-i|$ , for  $|j-i| < b$ .

The study of the overlap between of many-body states subjected to a perturbation has also been a traditional subject of investigation in nuclear physics problems<sup>29</sup>. More recently there is a renewed interest in examining overlaps among excited states<sup>30</sup>. This study is much more involved than ours, since the states considered are superpositions of Slater determinants, rather than a single one as studied here. A full theory for such a case is still lacking; available numerical evidence (evidently for small systems) indicates that the scaling of the overlaps with  $n$  follows a Gaussian, a fact which is yet to be explained.

## ACKNOWLEDGMENTS

We thank D. Kusnezov, I. V. Lerner, E. Mucciolo, M. Saraceno, and E. Vergini for helpful discussions. This work was supported by FAPERJ, CNPq and PRONEX (Brazil), and by the U.S.-Israel Binational Science Foundation, the DIP Foundation, the Minerva foundation and The Israel Science Foundation founded by the Israel Academy of Sciences-Center of Excellence Program (Israel).

## APPENDIX A: A PERTURBATION SERIES FOR $\log S$

In Section II we showed that the overlap of the ground states  $S$  can be written as  $S = \det A^{oo}$ , with the matrix

elements of  $A$  defined by Eq. (5). This is done for the case where time-reversal symmetry is present (absent), namely the orthogonal (unitary) symmetry. The notation “oo” stands for “occupied-occupied” states (in this Appendix we shall also use “oe” for “occupied-empty”). Within the Rayleigh-Schrödinger perturbation theory the overlap matrix is expanded as

$$A = \mathbb{1} + \epsilon B + \epsilon^2 C + \epsilon^3 D + \dots \quad (\text{A1})$$

Since  $AA^\dagger = \mathbb{1}$ , i.e., using the fact that this series is normalized, it is implied that

$$\begin{aligned} B + B^\dagger &= 0 \\ C + C^\dagger + BB^\dagger &= 0 \\ D + D^\dagger + CB^\dagger + BC^\dagger &= 0, \end{aligned} \quad (\text{A2})$$

etc.. In particular, one knows from perturbation theory that the first order correction  $B$  is an antihermitian matrix satisfying  $B_{ii} = 0$  and

$$\epsilon B_{ij} = \frac{\delta H_{ij}}{E_j - E_i}, \quad \text{for } j > i. \quad (\text{A3})$$

To obtain a perturbative series for  $\log |S|$  we use Eq. (A1) and the identity  $\log \det = \text{tr} \log$  to write

$$\log \det A^{\text{oo}} = \text{tr} \log (\mathbb{1} + \epsilon B^{\text{oo}} + \epsilon^2 C^{\text{oo}} + \epsilon^3 D^{\text{oo}} + \dots). \quad (\text{A4})$$

By expanding the logarithm and regrouping the terms in the sum order by order in  $\epsilon$ , we obtain

$$\log \det A^{\text{oo}} = \text{tr} \left[ \epsilon B^{\text{oo}} + \epsilon^2 (C^{\text{oo}} - \frac{1}{2} B^{\text{oo}2}) + \dots \right]. \quad (\text{A5})$$

The linear term in  $\epsilon$  vanishes since  $B_{ii} = 0$ . Using the first two equations in (A2) one arrives at

$$\log \det A^{\text{oo}} = -\frac{1}{2} \epsilon^2 \text{tr} (B^{\text{oe}} B^{\text{oe}\dagger} - C^{\text{oo}} + C^{\text{oo}\dagger}) + \mathcal{O}(\epsilon^3). \quad (\text{A6})$$

The contribution from  $C^{\text{oo}} - C^{\text{oo}\dagger}$  being purely imaginary corresponds to a phase in  $\det A^{\text{oo}}$ , so that

$$\log |\det A^{\text{oo}}| = -\frac{1}{2} \epsilon^2 \text{tr} B^{\text{oe}} B^{\text{oe}\dagger} + \mathcal{O}(\epsilon^3). \quad (\text{A7})$$

If we average over the parametric random matrix ensemble, Eq. (18), the third order terms disappear:

$$\langle \log |\det A^{\text{oo}}| \rangle = -\frac{1}{2} \epsilon^2 \text{tr} \langle B^{\text{oe}} B^{\text{oe}\dagger} \rangle + \mathcal{O}(\epsilon^4), \quad (\text{A8})$$

or, equivalently,

$$\langle \log |\det A^{\text{oo}}| \rangle = -\frac{1}{2} \sum_{ij} \left\langle \frac{|\delta H_{ij}|^2}{(E_j - E_i)^2} \right\rangle + \mathcal{O}[(\delta H)^4], \quad (\text{A9})$$

where  $j$  and  $i$  run over the occupied and empty states, respectively.

This calculation also shows that

$$\exp \langle \log |\det A^{\text{oo}}| \rangle - \langle |\det A^{\text{oo}}| \rangle = \mathcal{O}(\epsilon^4). \quad (\text{A10})$$

## APPENDIX B: GRAND CANONICAL AVERAGES

In this appendix we study a slightly different question, complementary to the ones we have addressed so far. It is related to the averaging procedure. Suppose we have an ensemble of systems, each of which having a given number of electrons,  $N$ , which is kept fixed as the parameter  $X$  is varied. Let us assume, though, that the *preparation* of this ensemble of systems is performed *grand canonically*, i.e., by attaching each sample to a weakly coupled particle reservoir at a given chemical potential  $\mu$ , equilibrating, and then removing this coupling. The number of electrons in each system may vary, but is kept fixed during the “measurement” (i.e., varying  $X$ ). This procedure has been defined in Refs. 26,23 as *grand-canonical—canonical*. Under these conditions we employ a grand-canonical averaging scheme to calculate  $\langle \log |S| \rangle$ . Here we expect that large fluctuations due to avoided crossings will be suppressed, since the statistical weight of an avoided crossing needs to be modified from  $P(s)$  (canonical) to  $sP(s)$  (grand canonical)<sup>22</sup>. This reflects the fact that the probability to place the chemical potential in a given gap (between the last occupied and the first vacant level) is proportional to the size of the gap.

The results of our simulations using the grand canonical ensemble are summarized by Fig. 6. There, as in Fig. 2, we show  $\langle \log |S| \rangle$  and its different approximation schemes (explained in Section IV) as a function of  $N$ .

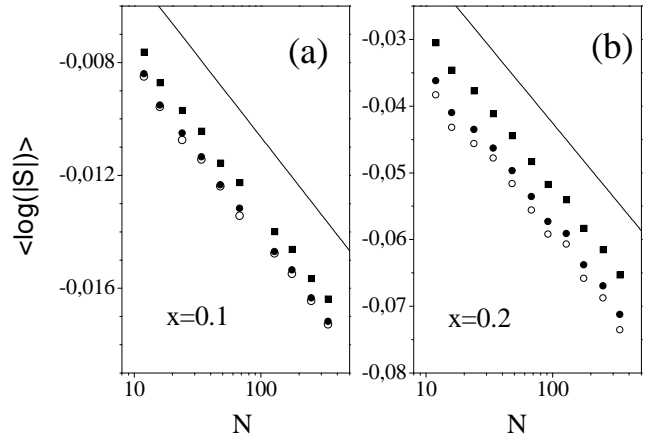


FIG. 6. The average  $\log |S(x)|$  as a function of  $N$ . The number of realizations for each  $N$  is  $M = 10^4$  and (a)  $x = 0.1$  and (b)  $x = 0.2$ . Open dots stand for the exact  $\langle \log |S| \rangle$ , filled dots for  $\langle I_{\text{norm}} \rangle$ , squares for  $\langle I \rangle$ , whereas the solid lines represent  $\langle \tilde{I} \rangle$ . See Section IV for the definitions.

By comparing the results of Fig. 2 with the ones shown above we observe that the values of  $\langle \log |S| \rangle$ , as well as  $\langle I_{\text{norm}} \rangle$  and  $\langle I \rangle$ , obtained by the canonical simulation are systematically reduced with respect to the ones obtained using the grand canonical averaging procedure. This is in line with the reasoning that the grand canonical averaging suppresses large fluctuations corresponding to small gaps. Thus it eliminates the long small  $|S|$  tails of  $P(|S|)$  characteristic of the canonical ensemble for  $x \ll 1$ . We also observe that both ensemble averaging procedures tend to render similar results as the value of  $x$  is increased. (For this reason we refrain from showing the grand canonical averages corresponding to  $x = 0.5$  and  $x = 1.0$  as depicted in Fig. 2.)

Figure 7 quantifies the discussion presented in the foregoing paragraph. The object of study is the standard deviation  $\delta \log |S| = [\langle (\log |S|)^2 \rangle - \langle \log |S| \rangle^2]^{1/2}$ . For a fixed matrix size  $N = 50$  and  $M = 10^4$  realizations we compute the ratio  $R$  between the canonical and the grand canonical  $\delta \log |S|$  as a function of  $x$ . As expected  $R(x) > 1$  for all investigated values of  $x$ . Furthermore, as we increase  $x$  the occurrence of small gaps becomes less important and the canonical fluctuations get closer to the grand canonical ones.

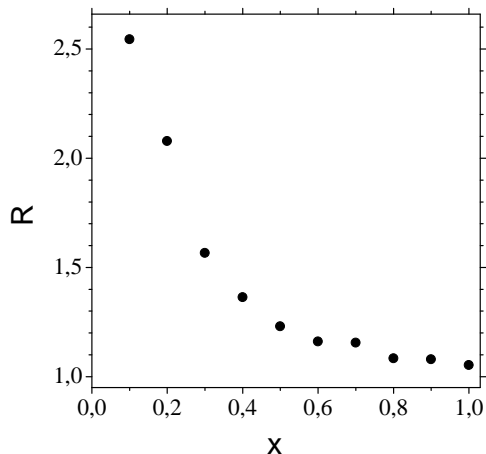


FIG. 7. The ratio between canonical and grand canonical standard deviation  $\delta \log |S(x)|$  as a function of  $x$  for a fixed  $N = 50$  and  $M = 10^4$ .

### APPENDIX C: ACCURACY OF THE APPROXIMATIONS FOR THE AVERAGE OF SINGLE PARTICLE OVERLAPS

Here we exhibit a test of the combination of first order perturbation theory and an average spectrum to account for averages of single particle overlaps. We want to compare the average

$$\langle |A_{N/2, N/2+j}|^2 \rangle = \langle |\langle \psi_{N/2}(X) | \psi_{N/2+j}(X + \delta X) \rangle|^2 \rangle \quad (\text{C1})$$

with the approximation discussed in Section IV

$$\langle |\tilde{A}_{N/2, N/2+j}|^2 \rangle = \frac{\beta x^2 \Delta^2}{2 \langle \varepsilon_{N/2+j} - \varepsilon_{N/2} \rangle^2}. \quad (\text{C2})$$

The quantity plotted in Fig. 8 is the ratio  $R = \langle |A_{N/2, N/2+j}|^2 \rangle / \langle |\tilde{A}_{N/2, N/2+j}|^2 \rangle$ . For  $j$  small as compared to  $N/2$  the average semi-circle spectrum can be approximated by a “picket fence” with spacing  $\Delta$ , meaning that  $\langle \varepsilon_{N/2+j} - \varepsilon_{N/2} \rangle^2 = j^2 \Delta^2$ . The ratio  $R$  is then

$$R(j, x) = \frac{2j^2}{\beta x^2} \langle |\langle \psi_{N/2}(X) | \psi_{N/2+j}(X + \delta X) \rangle|^2 \rangle. \quad (\text{C3})$$

The figure clearly displays the following features. For  $x$  fixed, the ratio  $R \rightarrow 1$  for large values of  $j$ . When  $x < 1$  the approximation works well except for the few states with, say,  $j \leq 5$ . In the case of  $j = 1$ , even if  $x \ll 1$ , perturbation theory breaks down due to very narrow avoided crossings.

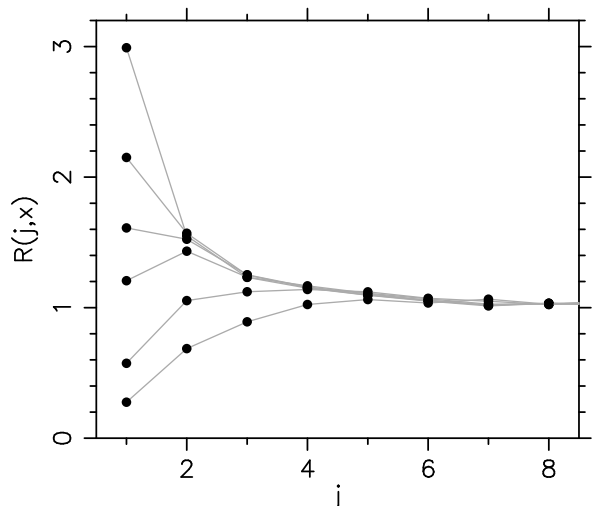


FIG. 8. Test of first order perturbation theory plus average spectrum. We plot the ratio  $R$ , the quotient “exact/approximate” (see text), as a function of the energy difference  $j$  for different values of the parametrical distance  $x = \delta X/X^*$  ( $x = 0.2, 0.3, 0.4, 0.5, 0.75, 1.0$ ; the curves with increasing  $x$  correspond to the ones with decreasing values for the first abscissa point  $j = 1$ ). Each curve was calculated by averaging over 10000 pairs  $(H_0, U)$  with  $N = 100$ .

<sup>1</sup> P. W. Anderson, Phys. Rev. Lett. **18**, 1049 (1967).

<sup>2</sup> L. P. Kouwenhoven, C. M. Marcus, P. L. McEuen, S. Tarucha, R. M. Westervelt, and N. S. Wingreen in *Mesoscopic Electron Transport*, edited by L. L. Sohn, L. P. Kouwenhoven, and G. Schön (Kluwer, Dordrecht, 1997)

- <sup>3</sup> Y. Alhassid, Rev. Mod. Phys. **72**, 895 (2000).
- <sup>4</sup> I. L. Aleiner, P. W. Brower and L. I. Glazman, cond-mat/0103008
- <sup>5</sup> E. Ben-Jacob and Y. Gefen, Phys. Lett. **108A**, 289 (1985); E. Ben-Jacob, Y. Gefen, K. Mullen, and Z. Schuss, Phys. Rev. B **37**, 7400 (1988).
- <sup>6</sup> M. L. Mehta, *Random Matrices*, 2nd Edition (Academic Press, New York, 1991).
- <sup>7</sup> T. Guhr, A. Müller-Groeling, and H. A. Weidenmüller, Phys. Rep. **299**, 190 (1998).
- <sup>8</sup> A. Kamenev and Y. Gefen, unpublished (1995).
- <sup>9</sup> Ya. M. Blanter, A. D. Mirlin, and B. A. Muzykantskii, Phys. Rev. Lett. **78**, 2449 (1997).
- <sup>10</sup> I. L. Kurland, I. L. Aleiner, and B. L. Altshuler, cond-mat/0004205.
- <sup>11</sup> T. Koopmans, Physica **1**, 104 (1934).
- <sup>12</sup> P. N. Walker, G. Montambaux, and Y. Gefen, Phys. Rev. B **60** 2541 (1999).
- <sup>13</sup> R. O. Vallejos, C. H. Lewenkopf, and E. R. Mucciolo, Phys. Rev. Lett. **81**, 677 (1998).
- <sup>14</sup> C. W. J. Beenakker, Phys. Rev. B **44**, 1646 (1991).
- <sup>15</sup> Y. Chen and J. Kroha, Phys. Rev. B **46**, 1332 (1992); I. L. Aleiner and K. A. Matveev, Phys. Rev. Lett. **80**, 814 (1998); I. E. Smolyarenko and B. D. Simons, unpublished.
- <sup>16</sup> B. L. Altshuler and B. D. Simons in *Mesoscopic Quantum Physics*, edited by E. Akkermans, G. Montambaux, J.-L. Pichard and J. Zinn-Justin (North-Holland, Amsterdam) p.1 .
- <sup>17</sup> Y. Alhassid and Y. Gefen, cond-mat/0101461.
- <sup>18</sup> Y. Alhassid and Y. Gefen, to be published.
- <sup>19</sup> M. Wilkinson, J. Phys. A **22**, 2795 (1989); Y. Alhassid and H. Attias, Phys. Rev. B **54**, 2696 (1996).
- <sup>20</sup> A. Szafer and B. L. Altshuler, Phys. Rev. Lett. **70**, 587 (1993).
- <sup>21</sup> B. D. Simons and B. L. Altshuler, Phys. Rev. Lett. **70**, 4063 (1993).
- <sup>22</sup> B.I. Shklovskii, Pis'ma Zh. Eksp. Teor. Fiz. **36**, 287 (1982) [JETP Lett. **36**, 352 (1982)].
- <sup>23</sup> A. Kamenev and Y. Gefen, Phys. Rev. B **49**, 14474 (1994); A. Kamenev and Y. Gefen in *Quantum Dynamics of Sub-micron Structures*, edited by H. A. Cerdeira *et. al.* (Kluwer Academic Publ., The Netherlands, 1995) pp. 81.
- <sup>24</sup> Y. Gefen, R. Berkovits, I. V. Lerner, and B. L. Alshuler, to be published.
- <sup>25</sup> A. Bohr and B. R. Mottelson, *Nuclear Structure*, vol. 1 (W. A. Benjamin, New York, 1969).
- <sup>26</sup> A. Kamenev and Y. Gefen, Phys. Rev. Lett. **70**, 1976 (1993).
- <sup>27</sup> M. Feingold and A. Peres, Phys. Rev. A **34**, 591 (1986).
- <sup>28</sup> D. Cohen, F. M. Izrailev, and T. Kottos, Phys. Rev. Lett. **84**, 2052 (2000); A. Barnett, D. Cohen, and E. J. Heller, Phys. Rev. Lett. **85**, 1412 (2000); D. Cohen, Ann. Phys. **283**, 175 (2000); D. Cohen and T. Kottos, Phys. Rev. E. **63**, 36203 (2001).
- <sup>29</sup> P. Ring and P. Schuck, *The Nuclear Many-Body Problem*, (Springer, New York, 1980).
- <sup>30</sup> D. Kusnezov, B. A. Brown, and V. Zelevinsky, Phys. Lett. B **385**, 5 (1996).